

GEOARCHAEOLOGY OF THE ANCIENT HARBOR SITE OF CAESAREA MARITIMA, ISRAEL: EVIDENCE FROM SEDIMENTOLOGY AND PALEOECOLOGY OF BENTHIC FORAMINIFERA

E. G. REINHARDT, R. T. PATTERSON AND C. J. SCHRÖDER-ADAMS

Ottawa-Carleton Geoscience Center and Department of Earth Sciences, Carleton University, Ottawa, Ontario, K1S 5B6, Canada

ABSTRACT

Foraminiferal analysis and ^{14}C dating of a core obtained from the entrance of the ancient harbor site of Caesarea Maritima, Israel provided paleo-environmental information which has enhanced previous archaeological interpretations. This integrated micropaleontological-sedimentological approach presents a new tool for solving marine archaeological problems.

Four distinct sedimentological units related to the harbor's history were recognized: preharbor deposits, harbor construction rubble, harbor and post harbor deposits. The sediments from the active harbor were characterized by mud, interrupted by intervals of coarse sand deposited during large low periodicity (25–50 years) storms. The area outside the harbor moles was continuously under the influence of wave action resulting in deposition of a coarse sandy substrate.

The sediment distribution corresponded with two distinct foraminiferal assemblages: Biofacies 1 was related to a low energy muddy substrate and was characterized by *Ammonia tepida*, *Cornuspira foliacea*, *Haynesina depressula* and *Triloculina subgranulata*; Biofacies 2 was related to a high energy sand substrate and was characterized by *Ammonia parkinsoniana* and *Porosonion granosum*.

Sedimentological and foraminiferal evidence as well as ^{14}C dates indicated that the mud was from the active harbor (commissioned in 21 BC) and that the harbor was no longer functioning according to its original design probably by the mid third century and definitely by no later than 490 AD. Previous research had suggested that the degradation of the harbor was most likely related to tectonic movement of the area. However, the timing of this event was not exactly known. Archaeologists have speculated that the Byzantine Emperor Anastasius I refurbished the harbor in the early 6th century. The results of this study have indicated that, even if this reconstruction did occur, the harbor was not returned to its original design or function.

INTRODUCTION

Ongoing archaeological studies at Caesarea, Israel are being carried out to determine the history of the ancient harbor. Anthropogenic activity, sedimentological, tectonic and meteorological patterns have had a profound influence on the environment and history of harbors. Since foraminifera are sensitive paleoenvironmental indicators, this site provided an excellent opportunity to test the application of micropaleontology and sedimentology to problems in marine archaeology. A combined micropaleontological and ar-

chaeological approach provided detailed information on the timing and nature of events which determined the history and state of the ancient harbor at Caesarea. To our knowledge, this was the first time any foraminiferal studies have ever been carried out in archaeological investigations of ancient harbors.

HISTORICAL CONTEXT

Caesarea is a historical site situated on the Israeli Mediterranean coast (34°53.5'E 32°30.5'N) midway between modern Tel Aviv and Haifa (Fig. 1 and Fig. 2).

In 21 BC, King Herod the Great, ruler of the Jewish state of Judea, commissioned an all weather harbor at Caesarea (Raban, 1992; Holum and others, 1988; Fig. 3). He hoped to ingratiate himself to the new ruler of Rome, Caesar Augustus, and at the same time to satisfy some of his economic needs (Owen, 1991). The construction of the harbor was difficult due to the natural constraints presented by the Israeli coastline. The coast is straight with no natural topography that could be expanded upon to build a harbor (Fig. 2; Raban and Hohlfelder, 1981). Herod's engineers however, succeeded in building an all-weather harbor by using hydraulic concrete, a new Roman building material, to form the breakwaters (Raban, 1989). Construction of the harbor took twelve years. Herod named the completed city Caesarea and the harbor Sebastos (Greek for Augustus; Raban, 1989).

Archaeological evidence has suggested that the city of Caesarea had a bustling harbor at least up to the mid- to late first century. However, there are indications that the harbor had problems as early as 66 AD (Holum and others, 1988) which may have been due to natural or man induced causes (Raban, 1989).

The Herodian breakwaters are presently submerged 5 m below the water surface (Fig. 1 and Fig. 4). The timing and exact mechanisms of this submergence have not been definitively described, although it is known that by 500 AD the harbor was in a poor condition (Hohlfelder, 1985; Hohlfelder, 1988; Raban, 1991; Raban, 1992). Procopius of Gaza, an early Christian bishop, wrote and complained to the Roman Emperor Anastasius I (491–518 AD) that the harbor was in a poor state; he used to watch ships wreck regularly in the exposed harbor (Raban, 1989). This report has been substantiated by the discovery of the remains of several shipwrecks on the harbor moles with diagnostic pottery sherds that have possible date ranges from the third to sixth centuries. At this point, the harbor breakwaters must have been under the waves, trapping some vessels trying to navigate over them (Raban, 1989). However, not long after Procopius account, Anastasius provided means by which the harbor could be refurbished (Raban, 1989; Raban, 1991; Raban, 1992; Oleson and others, 1984).



FIGURE 1. Aerial view of Caesarea with submerged rubble of ancient harbor breakwaters. Top of photograph is north.

The harbor at Caesarea had many forms during its history. The different morphologies were the result of human and natural alterations of the harbor structures and the coastal environment. The harbor was used in variable forms

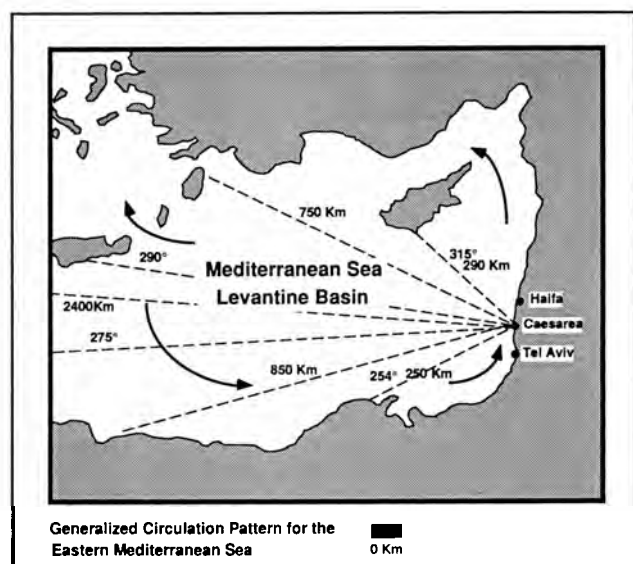


FIGURE 2. Generalized circulation pattern for the eastern Mediterranean Sea and generalized wave climate for the Israeli coast. Wave directions and fetch distances are shown (compiled from Cimerman and Langer, 1991; and Goldsmith and Golik, 1980).

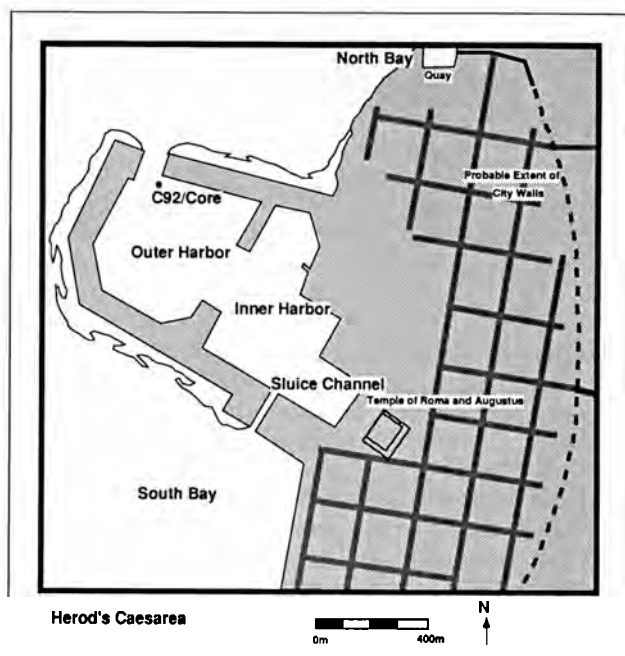


FIGURE 3. Representation of the probable configuration of Herod's harbor based on archaeological evidence, and the location of the core within its mouth (after Holum and others, 1988).

and capacities right up to the Crusader period (1265 AD) after which it was destroyed and abandoned (Holum and others 1988).

COASTAL GEOMORPHOLOGY

The Israeli Mediterranean coastline is dominated and determined by a series of Quaternary eolian sandstone ridges (kurkar) that run parallel to the coast. In several places, including Caesarea, continental loam beds (red hamra;

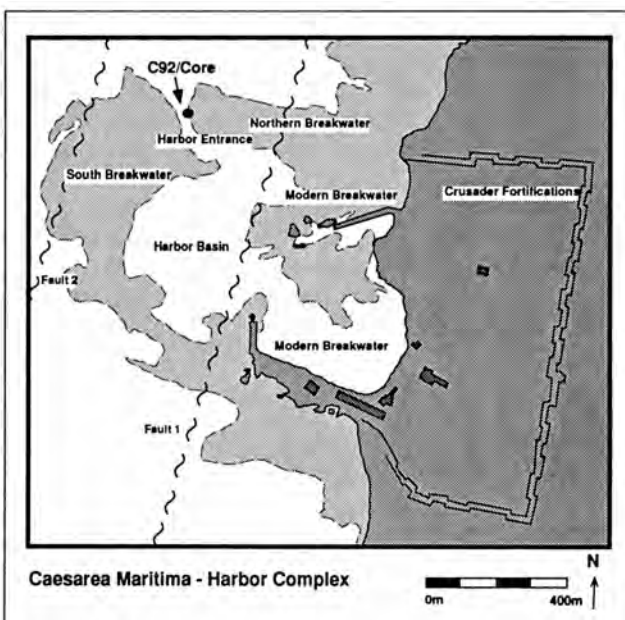


FIGURE 4. Modern representation of ancient harbor complex, showing location of core and the two major fault lines (after Holum and others, 1988).

Neev and others, 1987) outcrop both on land and below sea level. These loam beds have been associated with Quaternary sea level lowstands and oxidizing environments (Neev and others, 1987).

Caesarea is situated on the northern section of the central Israeli Mediterranean coast and is on the edge of the Nile littoral cell (Emery and Neev, 1960; Nir, 1980); (see Fig. 2). The principal sediments from the Nile were found to include silts and clays with a coarse sand-sized fraction that comprised 2–10% of the load (Nir, 1984; Raban, 1989). The Nile is the major source of clastic sediment for the eastern Mediterranean with 5–10% (350–700,000 m³/yr) of its yearly load of sand reaching the Israeli coast (Nir, 1984; Raban, 1989).

The wave climate for the Israeli coast has been summarized by Goldsmith and Golik (1980) who analyzed wave heights, periods, and directions at Ashdod between 1958–1965 (Fig. 2). They found that the largest wave heights (8 m) and periods (13 seconds) would occur once every 5–10 years and would approach in a narrow arc from 275° to 290° N due to maximum fetch distances. Sixty percent of the waves in the eastern Mediterranean would have a wave period of less than 6 seconds and heights less than 0.6 m, and would occur on an equal frequency between NW and SW directions. The remaining waves would occur mostly from the west and have periods between 7 and 11 seconds and heights between 0.6 and 2.1 metres.

The ancient harbor provided a unique quiet water environment on the coast which allowed accumulation of clay and silt sized sediment from the Nile and the coastal plain (Raban, 1989). The harbor protruded approximately 450 m from the natural shore and had an enormous effect on the sand transport and erosion of the local coastline. The harbor dammed northerly sand transport resulting in its accumulation south of the harbor. North of the harbor, a sand deficit and wave diffraction caused enormous coastal erosion, resulting in the truncation of the southern end of the high level aqueduct that runs parallel to the coast (Nir, 1985; Raban, 1989). Under calm sea conditions, the longshore current would have produced an eddy in the northern area just behind the harbor producing localized quiet water.

Evidence for what is thought to be a sluice channel was discovered on the southern promontory (Fig. 3). This sluice channel and perhaps others were constructed in order to create a flushing current within the harbor that would prevent silting (Hohlfelder and others, 1983). It has been postulated that the flushing, outflowing current was met by wave-driven water outside the harbor resulting in the deposition of silts and clays (Raban, 1989).

The exact width of the harbor entrance is not known since the area is now covered with rubble, but proposed widths range from 20–60 m (Raban, 1989). The large size (60 m) would have left the harbor open to northwest storms and the invasion of great amounts of sand. The narrow size (20 m) would have created difficulties with navigation, but would have produced a current flowing through the entrance that would have prevented sedimentation and kept the channel at the proper depth (Raban, 1983).

NEOTECTONIC HISTORY

Three faults have been recognized in the littoral zone running parallel to the coast in the area of Caesarea (Neev

and others, 1987). The fault closest to the shore has been found (Fig. 4), to correspond with a submarine cliff along the western abraded terrace, and is believed to have been active after the harbor was built. Two phases of faulting have been determined causing subsidence of the seaward downthrown block on both occasions (Neev and others, 1987). One of these seismic events, which probably occurred by the Early Byzantine period (4th century AD) as explained above (shipwrecks on the harbor moles), affected the harbor while it was still in use (Raban, 1989). The net downward movement of the offshore harbor structures resulting from these seismic events has put the western section of the harbor moles (150 m offshore) at 5 m below mean sea level and the shoreward section of the ancient harbor, which includes a sluice channel, just at sea level (Neev and others, 1987).

Various researchers have differing interpretations as to the timing and nature of the subsidence of the harbor moles and to the shoreline rebound during the two faulting phases (Raban, 1989; Neev and others, 1978; Neev and others, 1987). However, irrespective of interpretation, there is a definite 4–6 m elevational discontinuity when considering an east-to-west transect across the ancient harbor (Raban, 1989).

METHODS

CORING

A core was taken in the area of the harbor entrance. The sand overburden was removed by SCUBA divers with the use of an underwater dredge, exposing the harbor muds. The presence of large pieces of architectural rubble allowed the damming of the very mobile sand overburden, preventing it from flowing into the excavation area. Because this surface sand layer was active and highly mixed, a simple grab sample from the surface was obtained to represent the modern environment. Due to the nature of the archaeological deposits, the consistency of the mud, and the shallow water depth the sediment proved to be very difficult to core. A hand-held piston core was initially used, but due to the compact, dense nature of the mud and the inclusions of numerous pottery sherds it did not penetrate the sediment. A better method was devised which utilized (15 cm dia., 18 cm ht) metal casings manufactured from juice cans. These casings were able to penetrate the consolidated sediment, and due to their large diameter were generally not hindered by pottery, although some did hit larger pieces and did not penetrate very deeply (e.g. C92/Core 3 achieved only limited penetration into the coarse sand and was sampled as a whole). The casings were first hammered into the sediment. The underwater dredge was then used to remove sediment from around the casing. A thin piece of wood was then slid under the core and held in place by elasticized cords. The casing, sealed by the wood cover, was transported to the surface. Cores were obtained in this manner until a complete section was obtained. Between each successive core the area was cleaned using the dredge to eliminate any contaminating sediment. This resulted in a slight loss of sediment (~2 cm) between cores but prevented contamination. On the surface, the tops of the casings were removed and two opposing cuts made up the sides using tin snips.

The sediment core was cut in half by using a very fine wire, and logged.

Accurate elevations below mean sea level for the core were obtained by measuring distances below a known position (sighted using a shore based laser theodolite) on an overhanging architectural block.

LABORATORY METHODS

Samples of approximately 50 cc were shaken in tap water on a Burrell shaker until the clay was broken up and suspended. They were then washed under a 500 μ m sieve to remove coarse debris and then under a 63 μ m sieve to remove clay and silt.

The samples were divided using a dry splitter until an aliquot containing approximately 500 specimens was obtained. After quantitative analysis species counts were compiled and changed into relative percent abundances per sample.

The uncertainty for the counting errors were calculated using the methods proposed by (Patterson and Fishbein, 1989). Where the standard error is,

$$SX_i = [X_i(1 - X_i)/N]^{1/2} \quad (1)$$

where SX_i is the standard error; X_i is the estimated fractional abundance for each $i = 1, 2, 3 \dots I$ species; where I = (the total number of species in a particular sample); i is each species; and N is the total number of specimens counted in a sample. When making N counts the actual fractional abundance f_i lies between,

$$X_i - 1.96 SX_i \leq f_i \leq X_i + 1.96 SX_i \quad (2)$$

95% of the time regardless of the number of the species contained in the sample. The 95% confidence interval on

the estimated fractional abundances is therefore $X_i \pm 1.96 SX_i$.

Only 13 species were present in statistically significant numbers in at least one of the samples. Only these species were used for a Q-mode cluster analysis that was undertaken using the data, factor and cluster modules of Systat v. 2.1 (Wilkinson, 1987) on a Macintosh II cx (Table 1). The squared euclidean distances gave a measure of the proximity between cases, and the cases were arranged into a hierarchical dendrogram using Ward's linkage method (Fig. 5). This methodology has been shown to produce results similar to the statistically significant Error Weighted Maximum Likelihood (EWML) clustering method of Fishbein and Patterson (1993).

Selected specimens were mounted on a plug and coated with a palladium/gold mixture and examined on a Jeol JSM 6400 Scanning Electron Microscope at the Scanning Analytical Microscope Facility of Carleton University, Ottawa, Canada.

RESULTS

CORE SEDIMENTOLOGY

Each of the small cores were compiled to provide a total sedimentary section (Fig. 6). Unfortunately, due to the nature of the coring method some areas of the core were not recovered. The textures given are based on field descriptions and represent the dominant sediment size in the bed. Field examinations did not reveal any sedimentary structures within the mud units. The sand units also contained no sedimentary structures, except for oscillatory ripple structures in the sand interval just above the hamra section. However, in many of the beds there was evidence of de-

TABLE 1. Statistically significant species abundances (%) in samples from C92/core. Total representative percent is the sum of listed species. Top and bottom species' groups are from biofacies 1 and 2 respectively.

Species/Samples	C92/ Grab3	C92/24	C92/18	C92/15	C92/14	C92/ Core3	C92/30	C92/29	C92/28	C92/27	C92/39	C92/38	C92/37	C92/36	C92/35	C92/43	C92/45	C92/42	C92/46
Total Counts	470	476	1004	354	476	501	491	751	484	644	496	480	442	539	471	493	505	462	518
Depth Below MSL (m)	9.00	9.50	9.62	9.65	9.67	9.70	9.78	9.80	9.83	9.86	9.90	9.93	9.95	9.97	9.90	10.04	10.08	10.10	10.70
Biofacies	2	1	2	1	1	2	2	1	2	1	2	1	2	1	2	2	1	1	2
<i>Ammonia tepida</i>	0.21	12.39	11.35	9.04	8.19	1.60	5.09	6.66	10.74	7.76	4.44	7.71	7.47	8.16	7.64	4.06	13.66	11.47	0.39
<i>Cornuspira foliacea</i>	0.00	12.18	3.69	0.28	6.51	0.60	1.83	12.38	4.75	12.11	0.20	12.50	0.45	11.50	1.27	0.41	4.75	12.12	0.19
<i>Haynesina depressula</i>	0.00	11.55	8.17	7.63	14.92	0.20	3.26	9.45	7.64	10.09	1.61	10.63	3.62	12.24	4.88	1.62	4.75	6.06	0.00
<i>Pseudotriloculina sp. A</i>	0.00	2.10	1.39	0.00	3.36	0.00	0.41	3.60	2.27	3.73	0.40	4.58	1.36	3.53	0.21	0.00	1.39	0.87	0.19
<i>Quinqueloculina patagonica</i>	0.00	3.57	3.29	0.00	3.36	0.00	1.22	2.26	1.03	4.35	0.20	3.96	1.81	4.27	0.42	0.61	1.98	2.38	0.00
<i>Rosalina sp. A</i>	0.00	4.83	1.79	0.00	3.36	0.00	1.43	3.86	1.86	5.43	0.60	6.25	2.71	6.68	0.42	0.00	2.77	4.11	0.19
<i>Triloculina subgranulata</i>	0.00	14.92	17.83	0.28	11.34	0.20	4.89	17.71	10.33	13.66	2.62	15.21	4.75	13.54	5.31	3.85	11.09	15.15	0.00
<i>Ammonia parkinsoniana</i>	48.09	0.63	19.52	30.51	6.09	46.51	40.94	7.32	24.59	1.24	37.90	0.42	35.07	2.41	39.07	36.51	18.02	6.93	30.89
<i>Ammonia inflata</i>	4.68	0.00	0.80	1.13	0.00	2.59	1.02	0.53	1.03	0.00	3.02	0.21	1.36	0.00	2.76	1.01	0.00	0.22	2.32
<i>Elphidium craticulatum</i>	1.91	0.00	0.50	0.00	0.00	1.00	1.02	0.00	0.00	0.00	2.42	0.00	0.23	0.19	0.21	0.61	0.20	0.00	8.49
<i>Pararotalia spinigera</i>	10.64	0.00	0.00	0.00	0.00	0.40	1.02	0.00	0.00	0.16	5.44	0.00	0.00	0.00	0.00	13.79	0.59	0.22	0.00
<i>Porosonion granosum</i>	5.96	0.63	3.49	4.52	1.47	13.37	5.70	1.20	6.40	0.16	11.09	0.42	10.18	0.19	7.64	8.11	2.57	1.95	1.54
<i>Quinqueloculina sp. C</i>	1.06	0.21	0.50	0.28	0.00	4.39	0.81	0.00	0.21	0.00	2.82	0.00	0.00	0.00	1.49	1.22	0.00	0.43	8.30
Total repre- sentative %	72.55	63.03	72.31	53.67	58.61	70.86	68.64	64.98	70.87	58.70	72.78	61.88	69.00	62.71	71.34	71.81	61.78	61.90	52.51

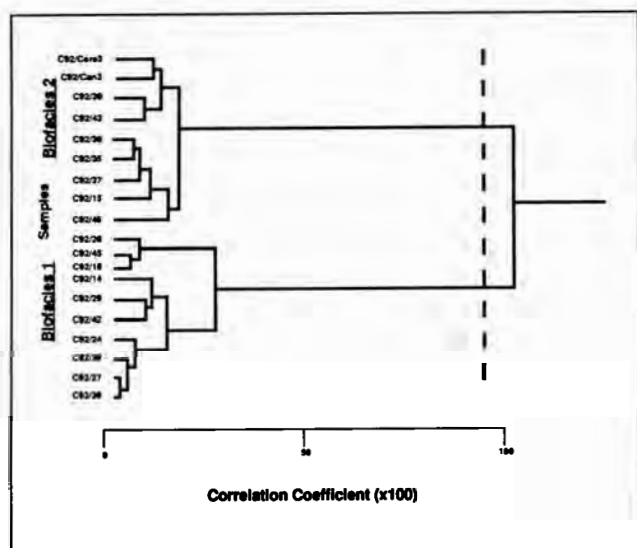


FIGURE 5. Q-mode dendrogram showing the nineteen samples from the C92/Core divided into two distinct Biofacies as indicated by the dashed line. Distinct clusters of samples with correlation coefficients greater than a selected level were considered Biofacies.

watering structures (deformed, convoluted bedding) that destroyed most primary features. The coarse sand beds contained little organic matter and were moderately to well sorted. The muddy deposits contained relatively high levels of organic matter and ranged from well to poorly sorted. Several distinct organic matter (OM) beds were also present and were characterized by an organic content of higher than 50%.

Through the section, five distinct sedimentary units were recognized. These are listed in descending order (Fig. 6): 1. Modern sand unit—typically moves from year to year and is very unstable. This interval contains mixed, well-rounded pottery. 2. Mud/sand unit—contains alternating mud and sand beds of various thickness, with organic layers. The pottery in this unit is very angular. 3. Architectural rubble—layer of cobble sized material and eroded pottery sherds. 4. Coarse sand—no pottery present. 5. Continental loam—hamra, soil reddish silty-clayey sand deposited in an oxidizing terrestrial environment (Neev and others, 1987).

BIOFACIES

Seventy-six different species of foraminifera were recognized in the 19 samples subsampled from the core (Appendix for taxon list). Two distinct biofacies were recognized through cluster analysis of the fractional abundances of the thirteen species present in statistically significant numbers. These biofacies showed a strong correlation to the alternating sedimentary textures recognized in the core (Table 1). Foraminiferal diversity was high in the muddy units and low in the coarse sand sediments.

Biofacies 1 was characterized by 7 species that displayed peak relative abundances in the mud and organic layers within the core. The most dominant species of this biofacies were *Cornuspira foliacea* (average abundance $9.37 \pm 4.45\%$), *Haynesina depressula* (average abundance $9.70 \pm 3.17\%$), and *Triloculina subgranulata* (average abundance $12.55 \pm 5.03\%$) (Fig. 7 and Table 2).

Biofacies 2 was characterized by 6 species which displayed relative peak abundances associated with coarse-grained textures. *Ammonia parkinsoniana* (average abundance $35.91 \pm 8.96\%$) and *Porosonion granosum* (average abundance $7.35 \pm 3.55\%$) were both characteristic of this biofacies.

Some of the 13 species present in statistically significant numbers did not display a distinct distribution pattern. For example, *Ammonia inflata* and *Pararotalia spinigera* had peak abundances in most coarse sand beds but were not present in all others (Table 1).

There were some anomalous clustering results as well (Fig. 5). These deviations were probably due to localized mixing of sediment and biota during deposition, or because of sediment dewatering which caused mixing, disrupting other sedimentary structures. For example sample C92/15 taken from a unit of high organic content, anomalously clustered with the coarse sand biofacies. This cluster affinity was due to a very low miliolid population in the sample, more characteristic of the coarse grained sand beds. Two other samples, C92/28 and C92/18 from sand units, fell out of the cluster. These samples were characterized by high abundances of miliolid species more typical of the mud units.

¹⁴C DATES

Radiocarbon dating was carried out at the IsoTrace Laboratory at the Accelerator Mass Spectrometry Facility of the University of Toronto (Table 3). The radiocarbon dates were the average of two machine ready targets measured on different occasions. Both the uncalibrated and the corrected dates are reported. The uncalibrated conventional results are dates stated in years before present, obtained using the Libby mean life of ¹⁴C of 8033 years. The uncertainty is the 68.3% confidence interval (Stuiver and others, 1986).

The two wood dates, ¹⁴C-1 and ¹⁴C-3, were corrected using dendrocalibration data and reported at the 95.5% confidence intervals. These two samples were obtained from both the top (9.6 m below m.s.l.) and the bottom (10.1 m below m.s.l.) of the core and delivered identical dates of 36 BC (Fig. 6), which preceded the building of the harbor (22 BC based on literary evidence). The identical dates obtained from both the top and bottom of the core suggested that the wood was derived from a similar source, and incorporated into the sediment at different times (such as wood from the wooden form-work used to construct the harbor moles). These two dates confirm that the deposits are from the Herodian harbor since the wood could not have occurred before the first century BC.

A third date was obtained from the uppermost organic layer. This layer proved to be a mixture of terrestrial and marine organic material. The uncalibrated date for this material was corrected for a terrestrial and then a marine origin. The marine calibration used a reservoir correction for the eastern Mediterranean of -80 ± 80 years (Stuiver and Reimer, 1993; Stuiver and Braziunas, 1993; Erol and Pirazzoli, 1992). Since the organic material was of mixed origin the date was reported as a range including at the 95.5% confidence interval, the lower limit of the terrestrial date and the upper limit of the marine date (197 BC–490

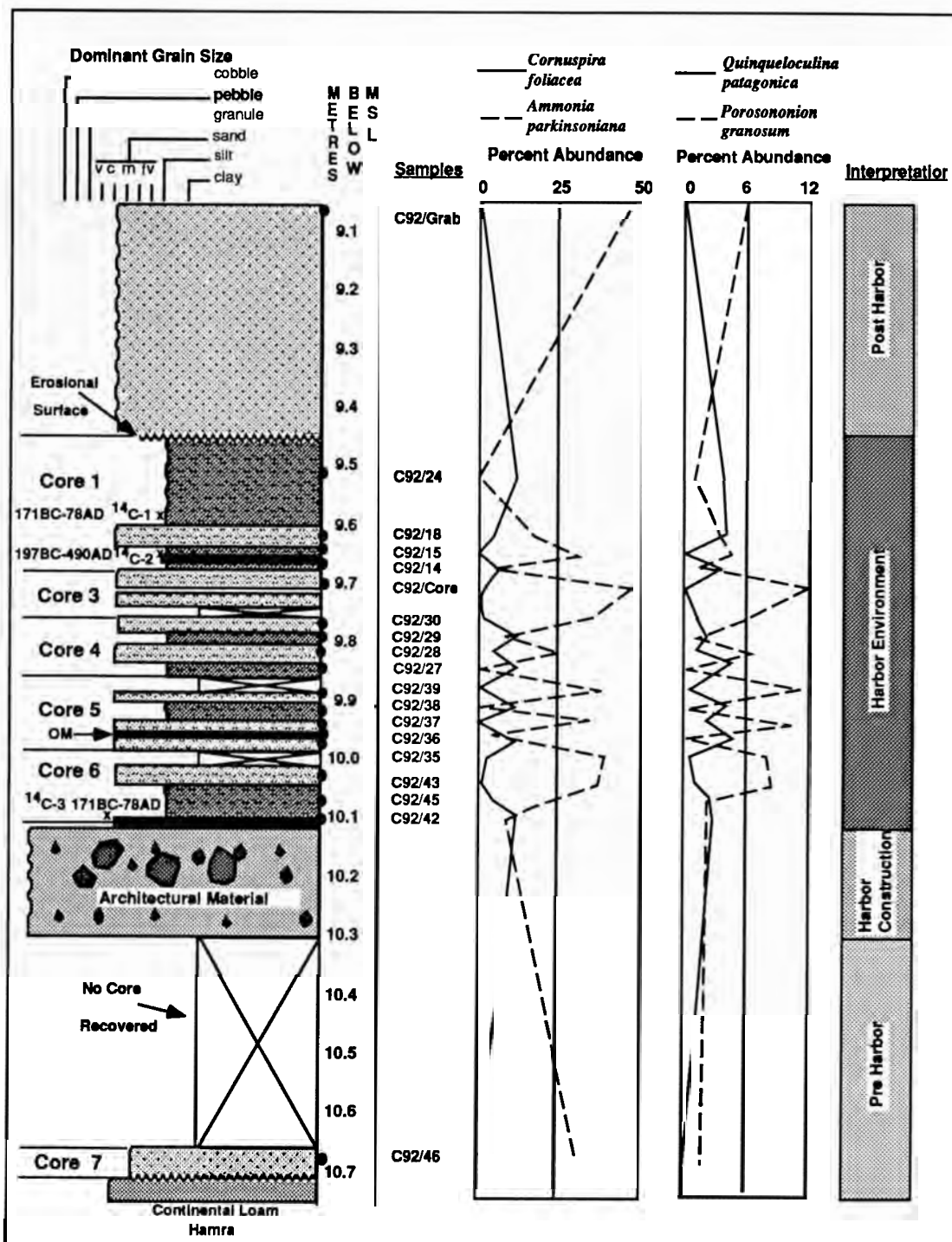


FIGURE 6. Compiled C92/Core from harbor entrance showing lithology, ¹⁴C dates, percent abundances of four common species and interpretation.

AD; Beukens-Isotrace Laboratory, oral communication, 1993).

DISCUSSION

HARBOR AGE

The date obtained for ¹⁴C-1, though very broad (197 BC–490 AD), offered the most information on the harbor's history. The fine marine and terrestrial vegetation material

used in the analysis, dictated that the resulting ¹⁴C date would be synchronous with deposition.

The broad range offered by the date was narrowed as the founding date for the harbor was well documented through literary evidence, the lower possible age limit of 197 BC was moved up to 10 BC. The upper age limit of the date was interpreted in two ways. One interpretation presumed that the organic material was 100% marine derived and that the true date was 2 standard deviations away from the reported

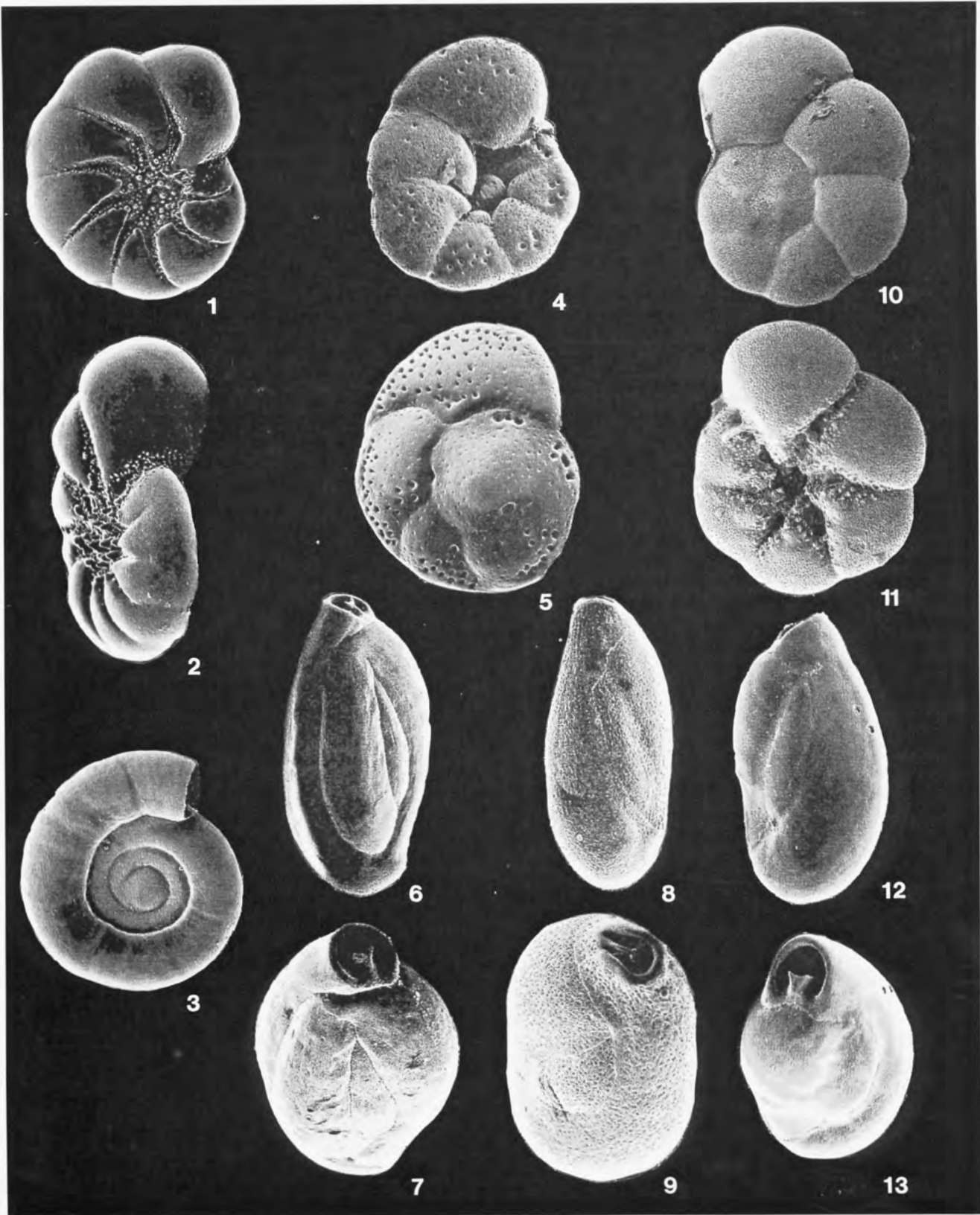


PLATE I

Biofacies 1: 1, 2 *Haynesina depressula* (Walker and Jacob, 1798). 1 Side view, $\times 230$. 2 Apertural view, $\times 350$. 3 *Cornuspira foliacea* (Philippi, 1844) side view, $\times 190$. 4, 5 *Rosalina* sp. A 4 Umbilical view, $\times 350$. 5 Spiral view, $\times 350$. 6, 7 *Quinqueloculina patagonica* (d'Orbigny, 1839). 6 Side view, $\times 300$. 7 Apertural view, $\times 420$. 8, 9 *Pseudotriloculina* sp. A. 8 Side view, $\times 245$. 9 Apertural view, $\times 385$. 10, 11 *Ammonia tepida* (Cushman, 1936). 10 Spiral view, $\times 230$. 11 Umbilical view, $\times 280$. 12, 13 *Triloculina subgranulata* d'Orbigny, 1839. 12 Side view, $\times 280$. 13 Apertural view, $\times 315$.

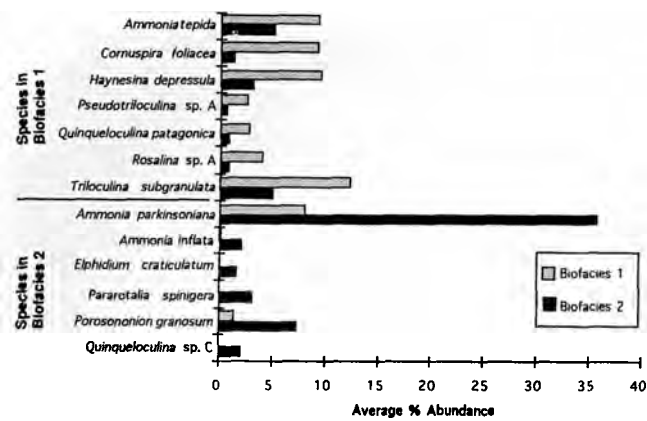


FIGURE 7. Bar graph showing the average percent abundance of species present in statistically significant numbers in each biofacies.

mean date. Using these criteria, the harbor was definitely no longer functioning in its original form after 490 AD.

A second interpretation presumed that the date was obtained from a mix of organic material derived from marine and terrestrial sources; therefore, it was probable that the harbor was no longer functioning in its original capacity sometime before the mid-third century (260 AD). This date correlated well with pottery dates (Late Roman-Byzantine, late second-early third centuries) obtained from other mud deposits found in the area of the harbor entrance (Raban 1992, Raban and others, 1990; Raban, 1989), with the finding of shipwrecks on the harbor breakwaters that had diagnostic pottery from the third century (Raban, 1989) and other land based archaeological evidence (Raban, 1992).

PALEOENVIRONMENTAL INTERPRETATION OF THE CORE

The core obtained from the harbor entrance included sediments deposited during the periods before the harbor was built, harbor construction, the active harbor, and after harbor destruction (Fig. 6). The results are discussed according to the chronological order of the core with greater emphasis placed on the active harbor sediments, as these were studied in the most detail.

The preharbor sediments were similar in their coarse texture and foraminiferal fauna (Biofacies 1—*Porosonion granosum*, *Ammonia parkinsoniana*) to sediments charac-

terizing the area today. Both modern and preharbor sediments were dominated by coarse sand sized material characteristic of a high energy environment. However, the modern environment included a large mass of archaeological rubble exposed above the substrate that provided localized hard grounds. Thus, the modern environment provided various new niches which were not present in preharbor times, resulting in some foraminiferal faunal differences.

The architectural layer was not sampled but contained large cobble-sized material with wave worn pottery material. This layer corresponded to constructional activity associated with the building of the harbor moles.

Inside the active harbor, water conditions were relatively quiet. The harbor acted like a sediment sink accumulating clays, silts and organic matter from: 1. local rain runoff in the city; 2. local wadis emptying into the Mediterranean to the south; and 3. the Nile with its high sediment load in conjunction with the general circulation pattern of the eastern Mediterranean. The quiet deposition within the harbor was interrupted only by the occasional violent storm coming either from a 275–290°N direction (max. fetch) or from the NW penetrating through the harbor entrance. In contrast, outside areas adjacent to the harbor were often affected by storms of every magnitude coming from all directions.

These contrasting water energy conditions resulted in a definite sediment cyclicity within the harbor. The slow accumulation of background mud deposits associated with a quiet water foraminiferal fauna (Biofacies 1) were interrupted by nine sand units and allochthonous foraminiferal faunas (Biofacies 2), deposited rapidly during infrequent storm surges. Following each storm incursion, the background sedimentation of cohesive clays and silts recommenced and recolonization of Biofacies 1 fauna occurred. The muds quickly dewatered and compacted (Nichols and Biggs, 1985) and would have been very hard to erode (Hjulstrom Diagram; Nichols and Biggs, 1985). These consolidated muds would then have protected the underlying uncohesive sand bed from further erosion. The sand layers had high pore water which increased in pressure as loading of successive beds occurred. As the pore water pressures increased the water was not permitted to exit the deposit due to the impermeability of the clay/silt layers above and below. Occasional ruptures in the mud units resulted in sand layers intruding into the clay/silt layer and disrupting sedimentary structures.

The cyclicity of sand units and the ^{14}C dates suggested that these storm events occurred approximately every 25–50 years and that there were no sudden changes in the harbor environment during its active life.

The foraminiferal biota (Biofacies 1) identified in the harbor muds was autochthonous and was characterized by a high miliolid (e.g. several *Quinqueloculina* spp. and *Triloculina* spp.) and *Ammonia* population typical of muddy Mediterranean lagoonal to normal marine environments which have variable salinities of 32–65‰ (Murray, 1991). The entrance of the active harbor represented a transitional environmental zone between lagoonal and normal marine conditions. The harbor mud also locally contained high concentrations of organic matter, which in the quiet depositional environment, produced locally anoxic conditions during decomposition. Biofacies 1 was associated with ideal

TABLE 2. Average percent abundance of each species in each biofacies with its respective standard deviation. Species groups are biofacies 1 and 2 respectively.

	Biofacies 1	Std	Biofacies 2	Std
<i>Ammonia tepida</i>	9.45	±2.44	5.30	±3.98
<i>Cornuspira foliacea</i>	9.37	±4.45	1.34	±1.63
<i>Haynesina depressula</i>	9.70	±3.17	3.10	±3.06
<i>Pseudotriloculina</i> sp. A	2.57	±1.55	0.62	±0.78
<i>Quinqueloculina patagonica</i>	2.90	±1.40	0.86	±1.05
<i>Rosalina</i> sp. A	4.14	±2.02	0.90	±0.97
<i>Triloculina subgranulata</i>	12.55	±5.03	4.98	±5.51
<i>Ammonia parkinsoniana</i>	8.17	±10.00	35.91	±8.96
<i>Ammonia inflata</i>	0.23	±0.38	2.06	±1.25
<i>Elphidium craticulatum</i>	0.04	±0.08	1.64	±2.53
<i>Pararotalia spinigera</i>	0.11	±0.20	3.13	±5.12
<i>Porosonion granosum</i>	1.46	±1.41	7.35	±3.55
<i>Quinqueloculina</i> sp. C	0.10	±0.16	2.08	±2.55

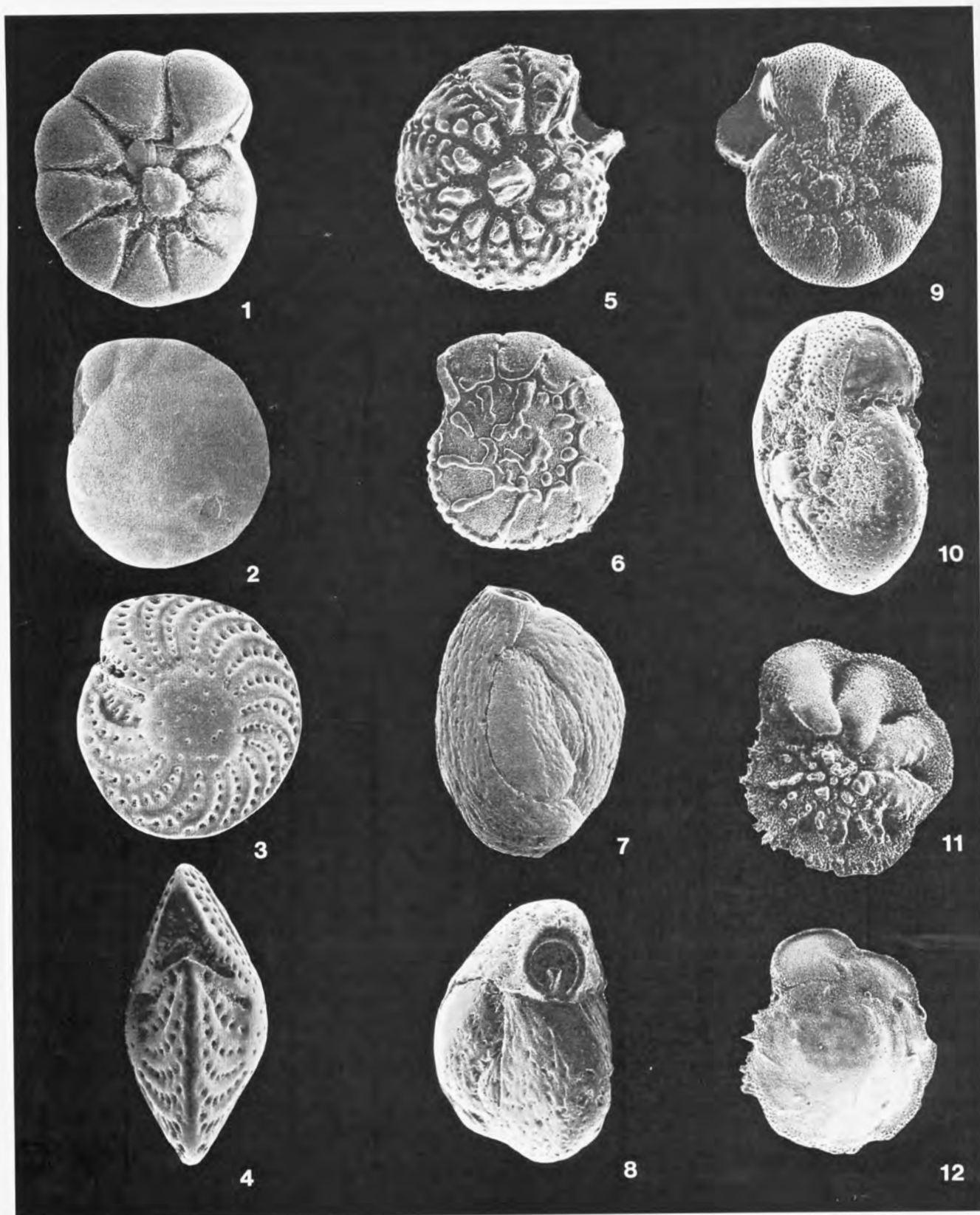


PLATE 2

Biofacies 2: 1, 2 *Ammonia parkinsoniana* (d'Orbigny, 1839) 2 Spiral view, $\times 100$. 1 Umbilical view, $\times 125$. 3, 4 *Elphidium craticulatum* (Fichtel and Moll, 1798) 3 Side view, $\times 100$. 4 Apertural view—last chamber broken, $\times 120$. 5, 6 *Ammonia inflata* (Seguenza, 1862) 5 Umbilical view, $\times 115$. 6 Spiral view, $\times 115$. 7, 8 *Quinqueloculina* sp. C 7 Side view, $\times 190$. 8 Apertural view, $\times 260$. 9, 10 *Porosonion granosum* (d'Orbigny, 1846) 9 Side view, $\times 160$. 10 Apertural view—last chamber broken, $\times 245$. 11, 12 *Pararotalia spinigera* (Le Calvez, 1949) 11 Umbilical view, $\times 100$. 12 Spiral view, $\times 100$.

TABLE 3. Radiocarbon dates obtained from wood and organic matter from the core.

Sample	Depth in Core (M) From MSL	Radiocarbon date (yrs B P)	Corrected Radiocarbon Date (Terrestrial)	95 5% Confidence Interval	Corrected Radiocarbon Date (Marine)	95 5% Confidence Interval	Laboratory Number	Dated Material
14C-1	9.60	2020 ± 50	36 BC	171 BC–78 AD	N/A	N/A	TO-3358	Wood
14C-2	9.65	2040 ± 60	50 BC	197 BC–77 AD	260 AD	30 AD–490 AD	TO-3357	Fine OM
14C-3	10.10	2020 ± 50	36 BC	171 BC–78 AD	N/A	N/A	TO-3444	Wood

environmental conditions, and had a high foraminiferal diversity with lower species abundances due to interspecific competition. Biofacies 2 was associated with poor environmental conditions, and as a result had a lower diversity but higher species abundances due to less interspecific competition.

The environmental transition between the low energy harbor and the higher energy conditions outside the harbor was not only exemplified by overall faunal changes but also by intraspecific ecophenotypic variation. In the core, distinct differences in distribution between the more compact *Ammonia parkinsoniana* and inflated *Ammonia tepida* types were recognized. Some researchers have presented evidence that *Ammonia parkinsoniana* and *Ammonia tepida* are end members of the same ecophenotypic cline (Poag, 1978; Wang and Lutze, 1986; Schnitker, 1974; Jorissen, 1988). The *Ammonia parkinsoniana* form was indigenous to the more open marine environment where conditions were harsher. The *Ammonia tepida* form characterized more restricted lagoonal habitats (such as found in a closed harbor basin environment) where conditions were more suitable for its development. *Ammonia tepida* dominated the mud beds (reflecting ideal conditions) while *Ammonia parkinsoniana* dominated the coarse sands (reflecting poor conditions). *Ammonia parkinsoniana* also had overall higher peak abundances than *Ammonia tepida* (average percent abundances: Biofacies 1 *Ammonia tepida* 9.45%; Biofacies 2 *Ammonia*

parkinsoniana 36%), which reflected overall species diversity.

The modern sediment and the sediment from the preconstruction period had high abundances of *Ammonia parkinsoniana* (48% and 46% respectively) and low *Ammonia tepida* abundances (0.21% and 0.39% respectively; Fig. 8). The samples in between these two intervals represented the period during which the harbor was present and active. Ecophenotypic variation existed only when the harbor and the contrasting open marine environment were present. This suggested that the modern and the pre-harbor environments were very similar and that a harbor environment did not exist during deposition of the lower sand unit.

CONCLUSIONS

The completion of the harbor at Caesarea in 10 BC, caused the local coastal environment to change from high to low energy in a matter of a decade. The local conditions reverted back to a high energy state probably before the mid third century and by no later than 490 AD. This chronology was based upon interpretation of ^{14}C dates, sedimentary textures and the foraminiferal fauna from a core taken in the entrance to the harbor. Four distinct environments were recognized: a preharbor stage, a construction stage, a harbor stage, and a post harbor stage.

The harbor stage was characterized by muddy back-

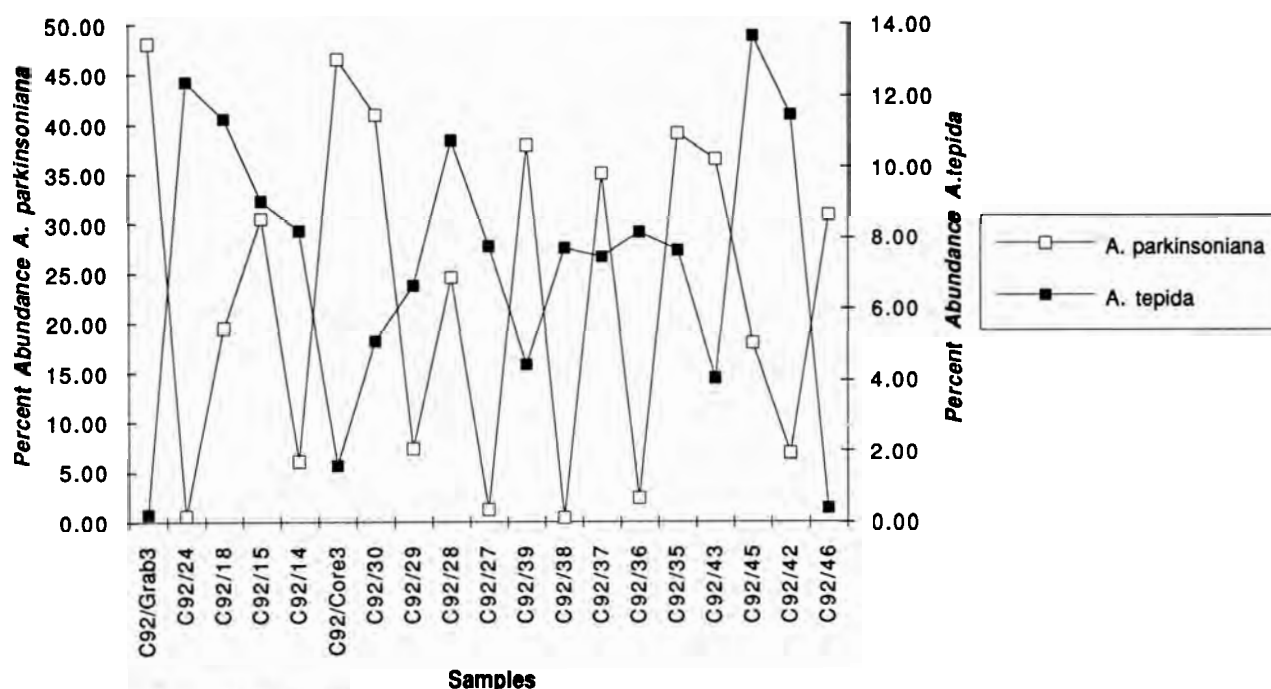


FIGURE 8. Percent abundance per sample of *Ammonia tepida* and *Ammonia parkinsoniana*. Samples are listed down core from left to right.

ground sedimentation that was interrupted by low periodicity storms (approximately 9 events) every 25–50 years. These storms either originated in the right direction (NW) which allowed the sand to intrude through the harbor entrance or were of such a magnitude (275°–290°—largest fetch distances) so as to breach the harbor breakwaters.

The harbor stage was also characterized by two foraminifera biofacies with *Ammonia parkinsoniana* and *Ammonia tepida* showing indicative ecophenotypic variation. The biofacies followed the general textures of the sediments, with water energy being the dominant controlling variable (Biofacies 1—low energy mud substrate; Biofacies 2—high energy sand substrate).

The decline of the harbor from its original form and function and cessation of mud and Biofacies 1 foraminiferal deposition was most likely related to the tectonics of the area. The results of this research have indicated that the harbor refurbishment done by Anastasius I in the early 6th century, did not return the harbor to its original form or function.

This integrated sedimentological–micropaleontological approach to a marine archaeological problem provided more detailed information than would otherwise be available from regular excavation techniques. The recovery of more cores from different areas within the ancient harbor may reveal a more detailed chronology of harbor use through comparisons and correlations of foraminiferal and sedimentological data.

ACKNOWLEDGMENTS

Research was partially supported by Natural Sciences and Engineering Research Council of Canada Research Grants: OGPOO41665 (to R.T.P.) and WFA0123127 to (C.J.S.-A.). We would like to thank Elwira Halicz (University of Jerusalem, Israel) for helping in the identification of the Mediterranean foraminiferal fauna, to Ray Buyce (Mercyhurst College, Erie, Pennsylvania) for devising an appropriate coring method and to Avner Raban (University of Haifa, Israel) and the Center for Maritime Studies for providing logistical support.

REFERENCES

- CIMERMAN, F., and LANGER, M. R., 1991, *Mediterranean Foraminifera*: Slovenian Academy of Science and Arts and Swiss Academy of Natural Sciences, 118 p.
- EMERY, K. O., and NEEV, D., 1960, Mediterranean Beaches of Israel: Bulletin of the Geological Survey of Israel, v. 26, p. 1–24.
- EROL, O., and PIRAZZOLI, P. A., 1992, Seleucia Pieria: an ancient harbour submitted to two successive uplifts: The International Journal of Nautical Archaeology, v. 21, p. 317–328.
- FISHBEIN, E., and PATTERSON, R. T., 1993, Error Weighted Maximum Likelihood (EWML): a new statistically based method to cluster quantitative micropaleontological data: Journal of Paleontology, v. 67, p. 475–486.
- GOLDSMITH, V., and GOLIK, A., 1980, Sediment transport model of the southeastern Mediterranean coast: Marine Geology, v. 37, p. 147–175.
- HOHLFELDER, R. L., 1985, Byzantine coin finds from the sea: A glimpse of Caesarea Maritima's later history, In: A. Raban (ed.), Harbor Archaeology, B.A.R. International Series, No. 257, Oxford p. 179–184.
- , 1988, Procopius' De Aedificiis 1.11, 1820: Caesarea Maritima and the building of harbours in late antiquity: Mediterranean Historical Review, v. 3, no. 1, p. 54–62.
- , OLESON, J. P., RABAN, A., and VANN, R. L., 1983, Sebastos Herod's harbor at Caesarea Maritima: Biblical Archaeology, v. 46, p. 133–143.
- HOLUM, K. G., HOHLFELDER, R. L., BULL, R. J., and RABAN, A., 1988, King Herod's Dream: Caesarea on the Sea: W. W. Norton & Company, New York, 244 p.
- JORISSEN, F. J., 1988, Benthic foraminifera from the Adriatic Sea; principles of phenotypic variation: Utrecht Micropaleontological Bulletin, v. 37, p. 1–174.
- MURRAY, J. W., 1991, Ecology and Palaeoecology of Benthic Foraminifera: Longman Group UK Limited, London, 397 p.
- NEEV, D., BAKLER, N., and EMERY, K. O., 1987, Mediterranean Coasts of Israel and Sinai: Taylor & Francis, New York, 125 p.
- , SCHACHNAI, E., HALL, J. K., BAKLER, N., and BEN-AVRAHAM, Z., 1978, The Young (Post Pliocene) Geological History of the Caesarea Structure: Israel Journal of Earth Sciences, v. 27, p. 43–64.
- NICHOLS, M. M., and BIGGS, R. B., 1985, Estuaries, In: R. A. Davis (ed.), Coastal Sedimentary Environments, New York, Springer-Verlag, p. 77–173.
- NIR, Y., 1980, Recent Sediments in Haifa Bay: Geological Survey of Israel, Report MG/11/80.
- , 1984, Recent Sediments of the Israel Mediterranean Continental Shelf and Slope: PhD dissertation, Goteborg University.
- , 1985, The Destruction of the Roman High Level Aqueduct, In: A. Raban (ed.) Harbour Archaeology: Proceedings of the First International Workshop on Ancient Mediterranean Harbours, Caesarea Maritima. British Archaeological Reports, Int. Series, v. 257, p. 185–194.
- OLESON, J. P., HOHLFELDER, R. L., RABAN, A., VANN, R. L., 1984, The Caesarea ancient harbor excavation project (CAHEP): preliminary report on the 1980–1983 seasons: Journal of Field Archaeology, v. 11, p. 281–305.
- OWEN, J., 1991, Sebastos—The Harbor of Caesarea Maritima; Investigation of Roman Harbor Technology: Unpublished Thesis, Tufts University, 124 p.
- PATTERSON, R. T., and FISHBEIN, E., 1989, Re-examination of the statistical methods to determine the number of point counts needed for micropaleontological quantitative research: Journal of Paleontology, v. 63, p. 245–248.
- POAG, C. W., 1978, Paired foraminiferal ecophenotypes in Gulf Coast estuaries: ecological and paleoecological implications: Transactions of the Gulf Coast Association Geological Society, v. 28, p. 395–421.
- RABAN, A., 1983, Guide to Sebastos: The Ancient Harbours of Caesarea Maritima. Tel Aviv: Schalg Publishing House 22 p.
- , 1989, Volume 1: The Site and the Excavations: The Harbours of Caesarea Maritima; Results of the Caesarea Ancient Harbour Excavation Project, part i & ii, 1980–1985, In: J. P. Oleson (ed.), BAR International Series 491, 516 p.
- , 1991, Sebastos: The royal harbour at Caesarea Maritima—a short living giant: Thracia Pontica, IV Sozopol.
- , 1992, Sebastos: The royal harbour at Caesarea Maritima—a short-lived giant: The International Journal of Nautical Archaeology, v. 21, no. 2, p. 111–124.
- , and HOHLFELDER, R. L., 1981, The ancient harbours of Caesarea Maritima: Archaeology, v. 34, no. 2, p. 56–60.
- , HOHLFELDER, R. L., HOLUM, K. G., STIEGLITZ, R. R., and VANN, R. L., 1990, Caesarea and its harbours: a preliminary report on the 1988 season: Israel Exploration Journal, v. 40, p. 241–256.
- SCHNITKER, D., 1974, Ecotypic variation in *Ammonia Beccarii* (Linné): Journal of Foraminiferal Research, v. 4, p. 217–223.
- STUIVER, M., PEARSON, G. W., and BRAZIUNAS, T., 1986, Radiocarbon age calibration of marine samples back to 9000 cal yr. BP: Radiocarbon, v. 28, p. 980–1021.
- , BRAZIUNAS, T. F., 1993, Modeling atmospheric ^{14}C influences and ^{14}C ages of marine samples to 10,000 BC: Radiocarbon, v. 35, p. 137–189.
- , and REIMER, P. J., 1993, Extended ^{14}C data base and revised calib 3.0 ^{14}C age calibration: Radiocarbon, v. 35, p. 215–230.
- WANG, P., and LUTZE, G. F., 1986, Inflated later chambers: ontogenetic changes of some recent hyaline benthic Foraminifera: Journal of Foraminiferal Research, v. 16, p. 48–62.

WILKINSON, L., 1987, SYSTAT: the System for Statistics: Evanston, IL: SYSTAT, Inc.

Received July 1993
Accepted September 1993

APPENDIX

A full list of species abundances is available from the authors on request.

TAXON LIST

- Adelosina* sp. A
Adelosina sp. B
Adelosina dubia = *Triloculina dubia* d'Orbigny, 1826
Ammonia inflata = *Rosalina inflata* Seguenza, 1862
Ammonia tepida = *Rotalia beccarii* var. *tepida* Cushman, 1936
Ammonia parkinsoniana = *Rosalina parkinsoniana* d'Orbigny, 1839
Amphistegina lobifera Larsen, 1976
Asterigerinata sp.
Asterigerinata mamilla = *Rotalina mamilla* Williamson, 1858
Biloculinella sp.
Bolivina sp. A
Bolivina sp. B
Brizalina sp. A
Brizalina sp. B
Brizalina sp. C
Bulimina elongata d'Orbigny, 1846
Cibicides sp. A
Cibicides variabilis d'Orbigny, 1839
Conorbella sp.
Cornuspira foliacea = *Orbis foliaceus* Philippi, 1844
Cycloforina tenuicollis = *Miliolina tenuicollis* Wiesner, 1923
Cycloforina sp. A
Cycloforina sp. B
Cycloforina sp. C
Cymbaloporeta sp.
Elphidium jensenii Cushman, 1905
Elphidium craticulatum = *Nautilus craticulatus* Fichtel & Moll, 1798
Elphidium gerthi Van Voorthuysen, 1957
Elphidium sp. A
Elphidium sp. B
Elphidium sp. C
Elphidium sp. D
Eponides sp.
Haynesina depressula = *Nautilus depressulus* Walker and Jacob, 1798
Hyalinonetrion gracillium = *Amphorina gracillima* Seguenza, 1862
Massilina sp.
Massilina gualtierana = *Quinqueloculina gualtierana* d'Orbigny, 1839
Miliolinella sp. A
Miliolinella sp. B
Miliolinella subrotunda = *Vermiculum subrotundum* Montagu, 1803
Neonorbina terquemi = *Discorbina terquemi* Rzehak, 1888
Nonionella opima Cushman, 1947
Nubeculina divaricata = *Sagrina divaricata* Brady, 1879
Pararotalia spinigera = *Globorotalia spinigera* Le Calvez, 1949
Porosonion granosum = *Noionina granosa* d'Orbigny, 1846
Porosonion poeyanum = *Polystomella poeyana* d'Orbigny, 1839
Pseudotriloculina sp. A
Pseudotriloculina sp. B
Pyrge sp.
Pyrgeella sphaera = *Bitiloculina sphaera* d'Orbigny, 1839
Quinqueloculina patagonica d'Orbigny, 1839
Quinqueloculina ungeriana d'Orbigny, 1846
Quinqueloculina sp. A
Quinqueloculina sp. B
Quinqueloculina sp. C
Quinqueloculina sp. D
Quinqueloculina sp. E
Rectuvigerina sp.
Rosalina sp. A
Rosalina sp. B
Rotalia sp.
Siphonaperta aspera = *Quinqueloculina aspera* d'Orbigny, 1826
Sorites sp.
Spirillina vivipara Ehrenberg, 1841
Spiriloculina sp.
Spirophthalmidium acutumargo = *Spiroloculina acutumargo* Brady, 1884
Triloculina sp. A
Triloculina sp. B
Triloculina sp. C
Triloculina sp. D
Triloculina sp. E
Triloculina sp. F
Triloculina subgranulata Cushman, 1918
Triloculina marioni Schlumberger, 1893
Triloculina affinis d'Orbigny, 1852
Varidentella sp.